



Mathematical Physiology Today: Examples of Synergies

Raymond Mejía

Laboratory of Cardiac Energetics, NHLBI, NIH, Bethesda, MD 20892-1061 USA, ray@helix.nih.gov

Abstract

We will illustrate advances in mathematical and computational biology during the past decade by showing advances in the mathematical modeling of physiological processes with emphasis on renal physiology. Access to mammalian and other genomes has provided fundamental information for the quantification and elucidation of biological phenomena. In addition, technological advances in measurement and analysis of experimental data make it possible to address physiological questions that have not been possible to study heretofore. We provide examples of synergies derived from these advances.

Keywords: mathematical biology, renal physiology, concentrating mechanism, proteomics, bioinformatics

1 Introduction

The state-of-the-art in mathematical and computational biology is presently advancing rapidly. The breadth of topics covered at the Gordon Research Conference on Mathematical and Theoretical Biology ([8], [9]) shows emerging, active areas of investigation. Topics in the 2004 Conference ([10]) included: systems biology, modeling transcriptional control in gene regulatory networks, biofluids and biological gels, motors and biological motion, innovations in theoretical immunology, neurobiology, spatial components in the modeling of ecological processes, and emergent species and diseases invasion. Several of these areas of investigation will influence significantly how we model biological phenomena. We describe advances in mathematical modeling in renal physiology that have resulted from developments in genomics, proteomics, bioinformatics and related technologies.

2 Models

Mathematical models of physiological processes have been successful at quantification and have provided insight into basic function. Nevertheless, in-vivo and in-vitro experiments often have limitations that restrict the ability to measure physical or physiological parameters required by models. However, techniques of molecular biology now permit indirect measurement of quantities that can complement physiological measurements. Access to these data is facilitated by databases and bioinformatics tools ([22]) that permit search and analysis by integrative biologists.

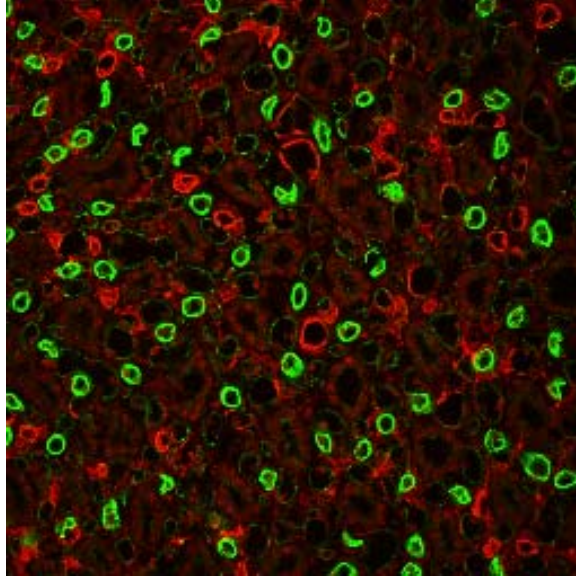


Figure 1: Section about 0.25 mm^2 taken approximately $50 \mu\text{m}$ from the tip of the rat papilla. AQP1 is labeled in green; ClC-K1 is labeled in red.

2.1 Urine Concentration

The ability of the mammalian kidney to produce a concentrated urine permits excretion of by-products of metabolism and retention of water and other solutes that are important to maintain homeostasis ([1]). The architecture of the rat kidney was first described by Kriz ([12]). Since then, the urine concentration mechanism of several species has been studied and modeled ([24], [25], [26], [27], [20], [13], [16]), but the mechanism is yet to be fully understood. The mechanism for generation of a concentration profile in the outer medulla is well understood, but the mechanism in the inner medulla is not ([29], [14]). Use of physiologic parameters measured in-vitro do not yield interstitial profiles observed in tissue slices and by micropuncture. Thus, models suggest that some parameters measured in-vitro are at variance with those in-vivo and models may not account for an important mechanism.

Microperfusion of dissected tubules has made it possible to measure transport rates in-vitro. The technique to microperfuse tubule segments in a bathing solution was pioneered by Orloff and Burg ([2]) in the mid 1960s to measure water and solute transport properties. By manipulating the composition of a bathing solution and the composition of the perfusate, measurement of the composition of the outflow permits calculation of the tubule's permeability to water and solutes. Modelers of the urine concentrating mechanism have used in-vivo measurements where available and in-vitro measurements as well as other approximations where necessary.

Microperfusion requires the ability to dissect renal tubules, and it has been especially difficult to dissect segments from the outer medulla of rodents. These segments are much less accessible than tubule segments in the renal cortex or the more distal inner medulla. Hence, transport parameters in nephron segments in the outer medulla have often been inferred from those of adjoining segments and from the histology of cells that form the tubes. In addition, tubule transport properties may vary along the length of lumen dissected,

while a perfusion experiment permits measurement of net transport in the segment perfused. Techniques of molecular biology [[7]] make it possible to label and identify transport proteins in portions of the kidney inaccessible for dissection. In addition, proteomic analysis used to measure proteins in tissues([28]) provides models with data obtained in various physiologic conditions.

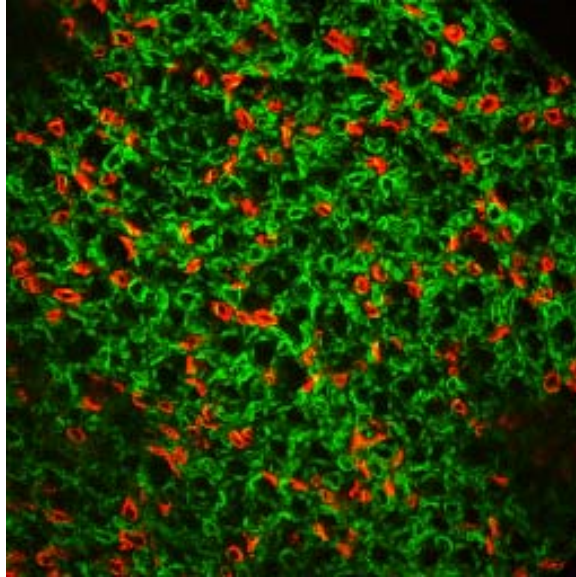


Figure 2: Section about 0.25 mm^2 taken at the junction of the inner and outer medulla. AQP1 is labeled in green; ClC-K1 is labeled in red.

2.2 Immunomorphometry

Low water permeability has been reported in deep inner medullary segments of chinchilla and rat ([4]). Recently, Mejia and Wade ([21]) have used immunofluorescent immunolabeling to label transporters in tissue sections of renal inner medulla. Table 1 shows the number of descending thin limbs (DTL), ascending thin limbs (ATL) and vasa recta (VR) labeled by antibodies for rat specific chloride channel protein (ClC-K1), aquaporin 1 (AQP1) and von Willebrand Factor (vWF) at various depths of the inner medulla. The number of loops of Henle decreases toward the tip of the medulla, and Table 1 shows that the fraction of descending limbs that express water transporter AQP1 decreases as well. Conversely, the fraction of DTL that label positive for ClC increases toward the tip. Moreover, thin limbs turning from descending to ascending have been shown to be labeled by ClC-K1 antibody on either side of the bend (Fig. 4 in [21]). The number of vasa recta labeled by vWF also decreases with proximity to the medullary tip due to reduced blood flow in the inner medulla.

Fig. 1 shows a section about 0.25 mm^2 taken about $50 \mu\text{m}$ from the tip of rat papilla. Chloride channel (ClC-K1) is labeled in red; aquaporin 1 (AQP1) is labeled in green. Since descending limbs turn below the section to return as ascending limbs, we infer that over 60% of descending limbs shown in this section are labeled by the ClC-K1 antibody. Fig. 2 is a section taken at the junction of the inner and outer medulla, where more loops are labeled and a larger fraction of DTL is shown to be AQP1 positive.

Distance to Tip μm	Labeled by <i>CIC</i> (<i>ATL</i>)	Labeled by <i>AQP1</i> (<i>DTL</i>) ²	Estimated <i>ATL</i> ¹ Incidence	% <i>DTL</i> with <i>AQP1</i>	Labeled by <i>vWF</i> <i>VR</i>
$0 < 200$ (3) ³	84 ± 27	5 ± 4	45 ± 13	11	35 ± 4 (2) ⁴
$200 < 400$ (7) ³	75 ± 23	14 ± 4	44 ± 12	32	46 ± 3 (3) ⁴
$400 < 900$ (12) ³	112 ± 22	31 ± 14	71 ± 18	44	43 ± 4 (3) ⁴
Junction IM-OM (3) ³	216 ± 21	97 ± 10	156 ± 15	62	74 ± 18 (2) ⁴
¹ $(AQP1 + CIC)/2$					
² <i>DTL</i> labeled by <i>AQP1</i> = structures labeled by <i>AQP1</i> – structures labeled by <i>vWF</i>					
³ (n) is average for n sections labeled for loops of Henle at this depth					
⁴ (n) is average for n sections labeled for vasa recta at this depth					

Table 1: Brattleboro rat tubules labeled and estimates of DTL, ATL and VR.

2.3 Kidney Model

A five-nephron population model ([20]), shown schematically in Fig. 3 and described in the Appendix, has been used to study the urine concentration mechanism. Transport parameters shown in Table 2 have been used to study changes in urine composition due to parameter changes along the nephron that are suggested by the immunomorphometric study described in the previous section. Water and NaCl permeabilities are modified near the turn in the loop of Henle relative to a control experiment. In the control experiment, water permeability (P_f) of long descending limbs (*DTL_{III}*) is taken to be uniform for each nephron population. In the turn experiment, water permeability is reduced to $11 \mu m/s$ and NaCl permeability is increased to $25 cm/s$ near the turn of the loop. A range of values for a parameter in the table means that the value varies as a function of nephron population. For example, P_f equal to 106–109 in *DTL_{III}* means a water permeability of $106 \mu m/s$ in populations 2 and 3 and $109 \mu m/s$ in populations 4 and 5. Other parameters are as in ([20]).

Fig. 4 shows NaCl mass flow in the collecting duct. The outflow of the collecting duct forms the urine, and NaCl excretion is shown to increase from $10 pmol/min$ in the control to $14 pmol/min$ in the turn experiment with reduced water permeability and increased NaCl permeability at the turn of the loops of Henle. Fig. 5 shows urea mass flow in the collecting duct, and urea excretion is shown to be equal in both experiments. Urine flow is shown to remain unchanged in Fig. 6.

2.4 Databases

Transport parameters that have been measured in several species under various physiologic conditions are available to modelers in the Renal Parameter Database (RPDB [23]). This database provides references to the literature where measurements are reported, summarizes the measurements, and describes experimental conditions under which measurements have been made. In addition, the database links physiologic parameters to regulatory and transporter proteins in the Collecting Duct Database (CDDB [15]).

For example, a search for AQP1 in the RPDB, Fig. 7, retrieves a record with title of publications, experimental measurements and more as shown in Fig. 8. The title is linked to the publication through Pubmed ([22]), and text words are linked as appropriate - see ‘water’ in Fig. 8. A request for more information in Fig. 8 returns a list with authors, year of publication and remarks about the measurements shown in Fig. 9. AQP1 is linked to additional information. A click on AQP1 in Fig. 9 retrieves a page, Fig. 10, from the CDDB ([15]) that links to AQP1 homologs in the human, rat and mouse genomes as well as to additional information about the protein. A click on water in Fig. 8 retrieves analogous data for all water transport

Segment	P_f $\mu m/s$	P_{NaCl} $cm/s \times 10^5$	P_{urea}	V_{NaCl}^m $pmol/mm/min$	K_{NaCl}^m mM
<i>PST</i>	141–109				
<i>DTL_{II}</i>	141–109				
<i>DTL_{III}</i>	106–109 (11)	0 (25)	90		
<i>ATL</i>		0 (25)	0–90	541–246	50
<i>TAL(OM)</i>				897–246	50
<i>TAL(MR)</i>				12	50
<i>CCD</i>	900			48	28
<i>OMCD</i>	900				
<i>IMCD_i</i>	510				
<i>IMCD_t</i>	510		75	46	28

Table 2: Transport parameters in the renal medulla are shown for the control and turn experiments (**bold font**).

proteins found to be expressed in the mammalian kidney (not shown).

This is a beginning in the effort to link protein expression under varying physiologic conditions to experimental measurements. Thus, proteomic analyses, illustrated by studies from Knepper’s laboratory ([17], [11], [28]) and the Elalouf laboratory ([6], [5]), can be used to provide integrated sets of data.

3 Conclusion

Mathematical biology is maturing rapidly as a field of scientific investigation stimulated in no small part by technological advances applied in the biological sciences. In particular, techniques in molecular biology and new discoveries about the genomes of many species permit us to postulate more realistic models.

Mathematical models of physiological processes benefit through the use of new techniques to obtain necessary data, and databases are making it possible to integrate several levels of observation. We have illustrated this by the use of immunofluorescent immunolabeling and of databases that integrate measurements that are used to obtain more realistic data for mathematical models.

4 Appendix

The model of the mammalian kidney ([20]) shown schematically in Fig. 3 consists of a well-mixed cortical interstitium, a medullary central core ([24], [25]) with highly permeable vasa recta and interstitium that form a single compartment, and five nephron populations. Fig. 3 shows a population of short nephrons that originate in the outer portion of the cortex and comprise approximately 70% of the nephrons in the rat and four populations of juxtamedullary nephrons that originate near the cortico-medullary boundary and extend into the inner medulla.

The differential equations that describe solute and water movement in the i th tube segment are as follows

$$\begin{aligned} \partial_t(A_i C_{ik}) + \partial_x F_{ik} &= -J_{ik} \\ F_{ik} &= F_{iv} C_{ik} - A_i D_{ik} \partial_x C_{ik} \end{aligned} \tag{1}$$

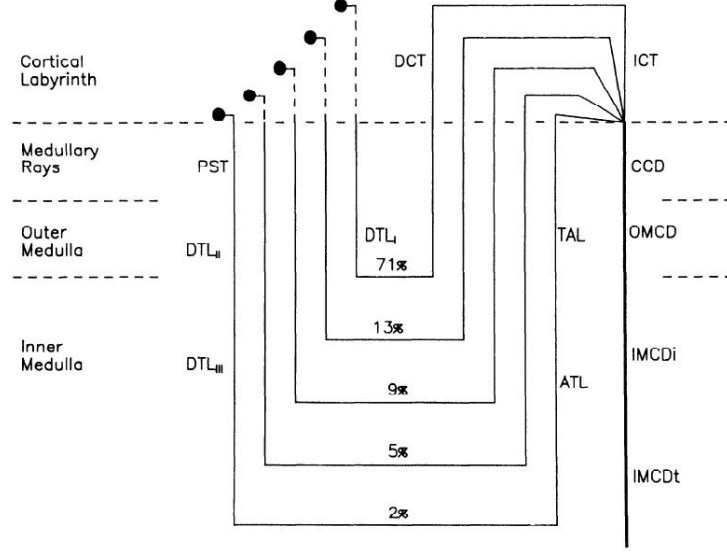


Figure 3: Schematic diagram of a five-nephron-population model. Short nephrons originate in the outer cortical labyrinth, while longer nephrons originate nearer the cortico-medullary border. PST is proximal straight tubule, DTL thin descending limb, ATL ascending thin limb. TAL thick ascending limb, DCT distal cortical tubule, CT connecting tubule, CCD cortical collecting duct, OMCD outer medullary collecting duct, IMCDi initial segment of inner medullary collecting duct, and IMCDt is the terminal segment of inner medullary collecting duct.

$$\partial_t A_i + \partial_x F_{iv} = -J_{iv} \quad (2)$$

$$\partial_x P_i = -R_{iv} F_{iv} \quad (3)$$

where t is time, I is the number of tube segments, and K is the number of solutes, with $1 \leq i \leq I$, and $1 \leq k \leq K$. A_i is the cross-sectional area of tube i ; C_{ik} is the concentration of the k th solute in the i th tube; x is axial distance along a tube, $0 \leq x \leq L_i$ with L_i the length of tube i . F_{ik} is mass flow, and J_{ik} is transmural solute flux of solute k in tube i . F_{iv} is volume flow in the axial direction in the i th tube; D_{ik} is the diffusion coefficient of the k th solute in tube i , and J_{iv} is the transmembrane water flux. P_i is the hydrostatic pressure, and R_{iv} is the resistance to flow in tube i .

Transmembrane solute and water fluxes are defined as

$$J_{ik} = 2\pi\rho_i P_{ik} \Delta C_{ik} + \frac{(1 - \sigma_{ik}) J_{iv} \Delta C_{ik}}{2} + J_{ik}^a$$

$$J_{iv} = -2\pi\rho_i P_{f,i} V_w \left[\sum_k \sigma_{ik} \Delta C_{ik} + \frac{P_q - P_i}{RT} \right]$$

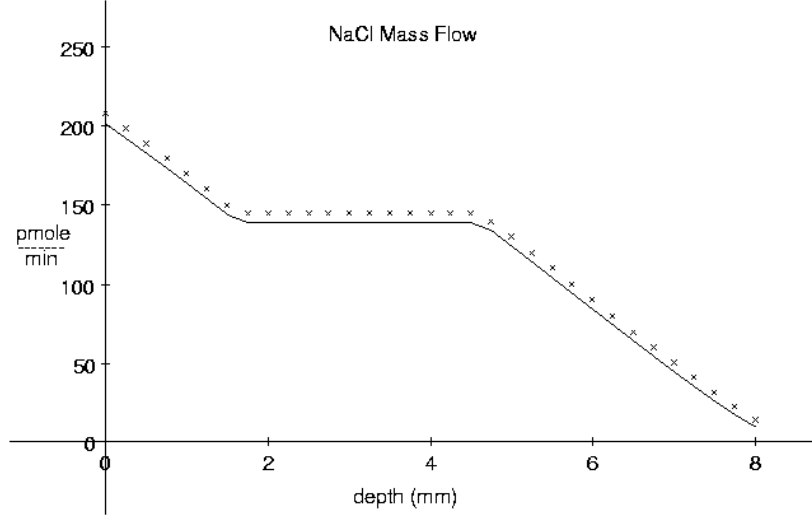


Figure 4: NaCl mass flow in the collecting duct is shown for (—) control and (x) turn experiments.

where ρ_i is the radius of tube i , P_{ik} is the permeability of the i th tube to the k th solute, and $\Delta C_{ik} = C_{ik} - C_{qk}$ with C_{qk} the concentration of the k th solute in the interstitium (subscript q). σ_{ik} is the Staverman reflection coefficient of the wall of the i th tube for the k th solute. Active solute transport is defined by Michaelis-Menten kinetics as $J_{ik}^a = V_{ik}^m C_{ik} / (K_{ik}^m + C_{ik})$ where V_{ik}^m is the maximum rate of transport, and K_{ik}^m is the half-maximal concentration. $P_{f,i}$ is the osmotic water permeability of tube i ; V_w is the partial molar volume of water; R is the gas constant, and T is absolute temperature.

Eqs. 1 – 3 are solved with the initial and boundary conditions described below. The equations are solved for each tube in the direction of flow with boundary conditions specified at the proximal end of each tube so that for $t \geq 0$

$$C_{1k}(0, t) = C_{1k}^o \text{ and } F_{1v}(0, t) = F_{1v}^o \quad (4)$$

with superscript o indicating a specified value and

$$C_{ik}(x_{ip}, t) = C_{(i-1)k}(x_{(i-1)d}, t) \quad (5)$$

for $1 \leq k \leq K$

$$F_{iv}(x_{ip}, t) = \pm F_{(i-1)v}(x_{(i-1)d}, t) \quad (6)$$

$$P_i(x_{ip}, t) = P_{(i-1)}(x_{(i-1)d}, t) \quad (7)$$

for $1 \leq i \leq I_h$ where I_h is the number of tubes in population h ; and ip and id signify the proximal and distal end of tube i , respectively.

In the cortex, the central core (subscript c) is considered to be a well-mixed bath with the concentration of each solute assumed equal to its concentration in plasma (superscript p), namely

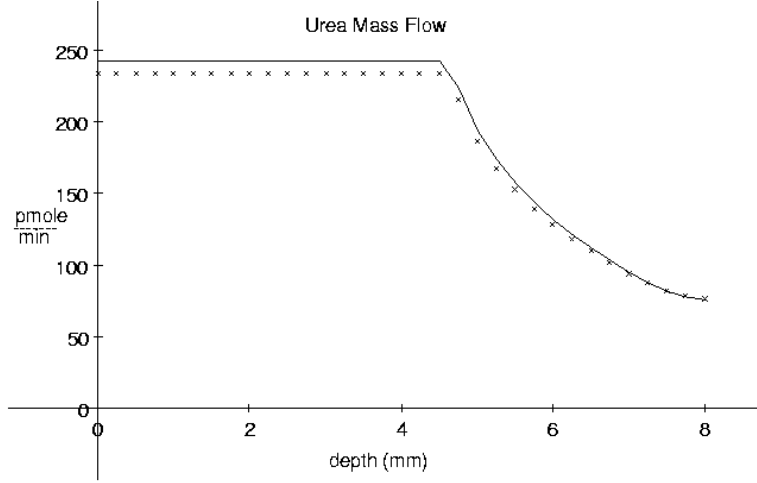


Figure 5: Urea mass flow in the collecting duct is shown for (—) control and (x) turn experiments.

$$C_{ck} = C_k^p \quad (8)$$

for $1 \leq k \leq K$ and the hydrostatic pressure is prescribed by

$$P_c = P_c^o \quad (9)$$

In the medullary rays and the medulla the central core is taken as a tube, closed at the papilla and open at the cortical labyrinth, through which other tubes exchange water and solutes. Boundary conditions for the medullary core are

$$\begin{aligned} F_{qk}(L_q, t) = F_{qv}(L_q, t) &= 0 \\ A_q(L_q)\partial_t C_{qk}(L_q, t) &= C_{qk}(L_q, t)J_{qv}(L_q, t) - J_{qk}(L_q, t) \\ P_q(0, t) &= P_c^o \end{aligned} \quad (10)$$

for $1 \leq k \leq K$ and $F_{qk} = F_{qv}C_{qk} - A_q D_{qk} \partial_x C_{qk}$. Mass and volume conservation require

$$\begin{aligned} J_{qk}(x, t) &= - \sum_i J_{ik}(x, t) \\ J_{qv}(x, t) &= - \sum_i J_{iv}(x, t) \end{aligned}$$

for $0 \leq x \leq L_q$ and all solutes k .

The initial conditions prescribed are as follows

$$C_{ik}(x, 0) = C_{ik}^o, \quad F_{iv}(x, 0) = F_{iv}^o, \quad P_i(x, 0) = P_i^o \quad (11)$$

for $0 \leq i \leq I$, $1 \leq k \leq K$, and axial position x .

Eqs. 1 – 3 are discretized using a second-order accurate finite difference method described in [19] and solved with boundary conditions Eqs. 4 – 10 and initial conditions Eqs. 11. The discretized equations are then solved using the parameter continuation algorithm described in ([18]).

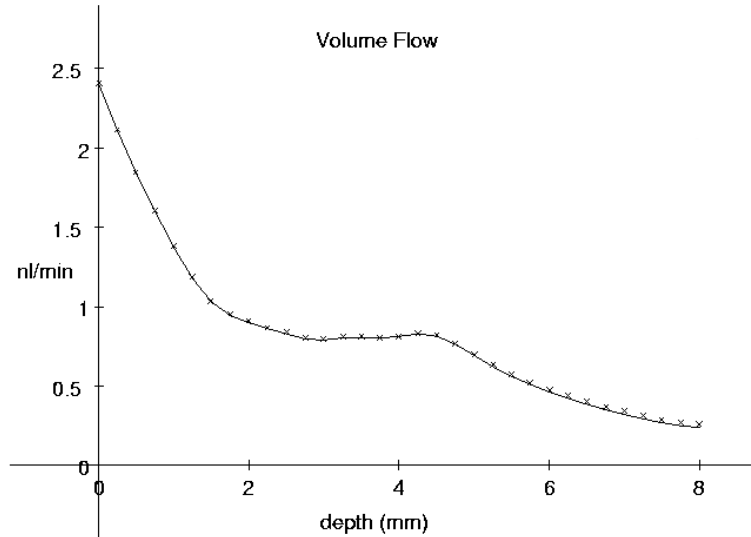


Figure 6: Volume flow in the collecting duct is shown for (—) control and (x) turn experiments.

Acknowledgments

I am grateful to many collaborators for their contributions. John L. Stephenson, who did seminal work in renal modeling, mentored and introduced me to the field. Mark A. Knepper has provided biological input and support. James B. Wade performed the immunofluorescent immunolabeling and lead the project on immunomorphometry. John Legato has been responsible for development and implementation of the databases. Chung-Lin (Joe) Chou and Robert A. Star have contributed through their continued advice and suggestions.

Division of Intramural Research

Bioinformatics Core Facility

Renal Parameter Database – Search Engine

The Renal Parameter Database has moved. You have been automatically forwarded to the new site. Please update your bookmarks. The new URL is: <http://cddb.nhlbi.nih.gov/rpdb>

Search Field: Search for:

We appreciate your feedback. If you have any comments or questions, please leave them using our [comment form](#).

Figure 7: Search window of Renal Parameter Data Base ([23]) shows a search for AQP1 in all search fields.

Division of Intramural Research

Bioinformatics Core Facility

The Renal Parameter Database has moved. You have been automatically forwarded to the new site. Please update your bookmarks. The new URL is: <http://cddb.nhlbi.nih.gov/rpdb>

Search Results

Title	Parameters
In vitro perfusion of chinchilla thin limb segments: segmentation and osmotic water permeability	Osmotic water permeability of rat distal inner medullary thin descending limb: 397 microns/s, Osmotic water permeability of outer medullary chinchilla long-loop thin descending limb: 2584 microns/s, Osmotic water permeability of the middle part of inner medullary chinchilla long-loop descending limb: 1520 microns/s, Osmotic water permeability of the distal 20% of the chinchilla long-loop descending limb: 50 microns/s, Osmotic water permeability of the thin ascending limbs from deep in the inner medulla: 0 microns/s, Raffinose permeability of chinchilla outer medullary descending limb: 6.5×10^{-5} cm/s, Raffinose permeability of chinchilla mid-inner medullary descending limb: 15×10^{-5} cm/s, Raffinose permeability of chinchilla outer medullary descending limb: 6.5×10^{-5} cm/s, Raffinose permeability of chinchilla mid-inner medullary descending limb: 15×10^{-5} cm/s, Raffinose permeability of chinchilla distal inner medullary descending limb: 9×10^{-5} cm/s, Raffinose permeability of chinchilla thin ascending limb: 22×10^{-5} cm/s

Figure 8: Result of the search shown in Fig. 7 includes publication title, parameters reported and a link to more information.

Department of Health and Human Services • National Institutes of Health
National Heart, Lung, and Blood Institute
PEOPLE • SCIENCE • HEALTH

• HOME • SITE INDEX • CONTACT US

Division of Intramural Research

Home » Information for Researchers » Division of Intramural Research » Collecting Duct Database » Renal Parameter Database - Search Results

TIPS ADVANCED SEARCH

Division of Intramural Research

Bioinformatics Core Facility

The Renal Parameter Database has moved. You have been automatically forwarded to the new site. Please update your bookmarks. The new URL is: <http://cddb.nhlbi.nih.gov/rpdb>

Search Results

Author	Year	Remarks
Chou CL, Knepper MA	1992	See AQP1 .

Figure 9: Shows authors, year of publication and remarks that link to AQP1 in CDDb ([15]).

Division of Intramural Research

Bioinformatics Core Facility

You may filter out proteins not known to be expressed in collecting duct, by checking the box, then pressing "Filter". To turn the filter off, uncheck the box then press "Filter" again.

Alternatively, you may highlight items known to be expressed in collecting duct. [Filter](#)

Transporters and Channels

Abbreviations	Name	Alternate names	Links
AQP1	aquaporin-1	-	        

1 Records found.

Key

-  [Search PubMed \(Only Collecting Duct\)](#)
-  [Search PubMed](#)
-  [Entrez Gene \(Human\)](#)
-  [Entrez Gene \(Rat\)](#)
-  [Entrez Gene \(Mouse\)](#)
-  [Online Mendelian Inheritance in Man](#)
-  [GeneCards: encyclopedia for genes, proteins and diseases](#)
-  [Rat Genome Database](#)
-  [Mouse Genome Informatics](#)

Figure 10: CDDB record links to AQP1 homologs in human, rat and mouse and detailed information about the protein.

References

- [1] Brenner, B.M. (Ed) Brenner and Rector's The Kidney. 7th ed., Saunders, Philadelphia 2004.
- [2] Burg, M., Grantham, J., Abramow, M., Orloff, J. Preparation and study of fragments of single rabbit nephrons. Am. J. Physiol. 1966 Jun;210(6):1293-8.
- [3] Chou, C.L., Knepper, M.A. In vitro perfusion of chinchilla thin limb segments: segmentation and osmotic water permeability. Am. J. Physiol. 1992 Sep;263(3 Pt 2):F417-26.
- [4] Chou, C.L., Knepper, M.A. In vitro perfusion of chinchilla thin limb segments: urea and NaCl permeabilities. Am. J. Physiol. 1993 Feb;264(2 Pt 2):F337-43.

- [5] Chabardes-Garonne, D., Mejean, A., Aude, J.C., Cheval, L., Di Stefano, A., Gaillard, M.C., Imbert-Teboul, M., Wittner, M., Balian, C., Anthouard, V., Robert, C., Segurens, B., Wincker, P., Weissenbach, J., Doucet, A., Elalouf, J.M. A panoramic view of gene expression in the human kidney. *Proc. Natl. Acad. Sci. USA.* 2003 Nov 11;100(23):13710-5.
- [6] Cheval, L., Virlon, B., Billon, E., Aude, J.C., Elalouf, J.M., Doucet, A. Large-scale analysis of gene expression: methods and application to the kidney. *J. Nephrol.* 2002 Mar-Apr;15 Suppl 5:S170-83.
- [7] Ecelbarger, C.A., Kim, G.H., Knepper, M.A., Liu, J., Tate, M., Welling, P.A., Wade, J.B. Regulation of potassium channel Kir 1.1 (ROMK) abundance in the thick ascending limb of Henle's loop. *J Am Soc Nephrol.* 2001 Jan;12(1):10-8.
- [8] Gordon Research Conferences.
<http://www.grc.uri.edu/>.
- [9] Gordon Research Conference on Theoretical Biology and Biomathematics.
<http://www.grc.uri.edu/scripts/cfml.exe?Template=/Jeff/makeconf.dbm>.
- [10] 2004 Gordon Research Conference on Theoretical Biology and Biomathematics.
<http://www.grc.uri.edu/programs/2004/theobio.htm>.
- [11] Knepper, M.A., Masilamani, S. Targeted proteomics in the kidney using ensembles of antibodies. *Acta Physiol. Scand.* 2001 Sep;173(1):11-21.
- [12] Kriz, W. The architectonic and functional structure of the rat kidney. *Z. Zellforsch Mikrosk. Anat.* 1967;82(4):495-535.
- [13] Layton, A.T., Layton, H.E. A region-based model framework for the rat urine concentrating mechanism. *Bull. Math. Biol.* 2003 Sep;65(5):859-901.
- [14] Layton, H.E., Knepper, M.A., Chou, C.L. Permeability criteria for effective function of passive counter-current multiplier. *Am. J. Physiol.* 1996 Jan;270(1 Pt 2):F9-20.
- [15] Legato, J., Knepper, M.A., Star, R.A., Mejia, R. Database for Renal Collecting Duct Regulatory and Transporter Proteins. *Physiol Genomics* 2003 Apr 16;13(2):179-81.
- [16] Marcano-Velázquez, M., Layton, H.E. An inverse algorithm for a mathematical model of an avian urine concentrating mechanism. *Bull. Math. Biol.* 2003 Jul;65(4):665-91.
- [17] McKee, J.A., Kumar, S., Ecelbarger, C.A., Fernandez-Llama, P., Terris, J., Knepper, M.A. Detection of Na(+) transporter proteins in urine. *J. Am. Soc. Nephrol.* 2000 Nov;11(11):2128-32.
- [18] Mejia, R. CONKUB - A conversational path-follower for systems of nonlinear equations. *J. Comput. Phys.* 1986 Mar;63(1):67-84.
- [19] Mejia, R., Stephenson, J.L. Solution of a multinephron, multisolute model of the mammalian kidney by Newton and continuation methods. *Math. Biosci.* 1984;68(2):279-298.
- [20] Mejia, R., Sands, J.M., Stephenson, J.L., Knepper, M.A. Renal actions of atrial natriuretic factor: a mathematical modeling study. *Am. J. Physiol.* 1989 Dec;257(6 Pt 2):F1146-57.

- [21] Mejia, R., Wade, J.B. Immunomorphometric study of rat renal inner medulla. *Am. J. Physiol. Renal Physiol.* 2002 Mar;282(3):F553-7.
- [22] National Center for Biotechnology Information. <http://www.ncbi.nlm.nih.gov/>.
- [23] Renal Parameter Database. <http://cddb.nhlbi.nih.gov/rpdb/>.
- [24] Stephenson, J.L. Concentration of urine in a central core model of the renal counterflow system. *Kidney Int.* 1972 Aug;2(2):85-94.
- [25] Stephenson, J.L. Concentrating engines and the kidney. II. Multisolute central core systems. *Biophys. J.* 1973 Jun;13(6):546-67.
- [26] Stephenson, J.L. Concentrating engines and the kidney. III. Canonical mass balance equation for multinephron models of the renal medulla. *Biophys. J.* 1976 Nov;16(11):1273-86.
- [27] Stephenson, J.L., Mejia, R., Tewarson, R.P. Model of solute and water movement in the kidney. *Proc. Natl. Acad. Sci. USA* 1976 Jan;73(1):252-6.
- [28] van Balkom, B.W., Hoffert, J.D., Chou, C.L., Knepper, M.A. Proteomic analysis of long-term vasopressin action in the inner medullary collecting duct of the Brattleboro rat. *Am. J. Physiol. Renal Physiol.* 2004 Feb;286(2):F216-24.
- [29] Wexler, A.S., Kalaba, R.E., Marsh, D.J. Passive, one-dimensional countercurrent models do not simulate hypertonic urine formation. *Am. J. Physiol.* 1987 Nov;253(5 Pt 2):F1020-30.